UC Irvine
UC Irvine Previously Published Works

Title

Raman scattering in V3Si, V3Ge, Nb3Sn, and Nb3Sb: Damping of the Eg optical phonon by interband electronic excitations

Permalink

https://escholarship.org/uc/item/3fq215dx

Journal

Physical Review B, 27(6)

ISSN

2469-9950

Authors

Dierker, SB
Merlin, R
Klein, MV
et al.

Publication Date

1983-03-15

DOI

10.1103/physrevb.27.3577

Peer reviewed

Raman scattering in V_3Si, V_3Ge, Nb_3Sn, and Nb_3Sb: Damping of the E_g optical phonon by interband electronic excitations

S. B. Dierker

*Materials Research Laboratory and Department of Physics, University of Illinois at Urbana-Champaign,
Urbana, Illinois 61801*

R. Merlin*

*Materials Research Laboratory and Coordinated Science Laboratory, University of Illinois at Urbana-Champaign,
Urbana, Illinois 61801*

M. V. Klein

*Materials Research Laboratory, Coordinated Science Laboratory, and Department of Physics,
University of Illinois at Urbana-Champaign, Urbana, Illinois 61801*

G. W. Webb and Z. Fisk

Institute for Pure and Applied Physical Sciences, University of California, San Diego, La Jolla, California 92093

We report measurements of the E_g optical phonon in V_3Ge, V_3Si, and Nb_3Sb, and of the T_{2g} optical phonon in Nb_3Sb measured from 9 to 400 K. The E_g optical phonon in V_3Ge has an anomalous width, shape, and temperature dependence, similar to that seen in V_3Si and Nb_3Sn. Both the E_g and T_{2g} optical phonons in Nb_3Sb, on the other hand, show no anomalous behavior and can be understood in terms of simple anharmonic interactions. We point out the existence of a linear correlation between the magnetic susceptibility and the E_g phonon linewidth for V_3Si, V_3Ge, and Nb_3Sn. Scaling arguments show that the E_g phonon linewidth of these three compounds exhibits very similar temperature dependences, with the remaining small differences yielding information concerning the distribution of the joint electronic density of states with respect to the Fermi level. These anomalies are attributed to coupling of the E_g phonon to interband electronic transitions between the flat bands emanating from the Γ_{12} level. A simple model of the interaction quantitatively reproduces the temperature dependence of the E_g phonon linewidth.

I. INTRODUCTION

The two early major theories of the martensitic transition in $A15$ compounds were advanced by Labbé and Friedel[1] and by Gorkov.[2,3] In the original Labbé-Friedel model, the structural instability is attributed to a second-order Jahn-Teller electronic instability. The Fermi level was placed very close to the bottom of triply degenerate Γ-point bands, which were split by the tetragonal distortion. The Gorkov model of the martensitic transition is based on the pseudo Peierls charge-density-wave— (CDW-) driven transition in a one-dimensional chain. The Fermi level was located close to doubly degenerate X-point bands, which were split by dimerization of the transition-metal atoms in the linear chains. In the Labbé-Friedel model, the electronic instability couples directly to the strain and hence indirectly to the E_g optical phonon; in the Gorkov model, the electronic instability couples directly to the E_g opti-

cal phonon and hence indirectly to the strain. However, despite considerable success in accounting for the anomalous properties of $A15$ compounds, these models and their subsequent variants[4-8] all suffer from the problem of being based on simplified, essentially one-dimensional models of the electronic band structure. Early band-structure calculations by Mattheiss[9] showed that interchain coupling is strong enough that the one-dimensional character of the bands is essentially wiped out; there is no threefold degeneracy in the bands at the Γ point near the Fermi energy, nor is the X-point degeneracy (required by symmetry of the $A15$ structure) located near the Fermi energy. This led Bhatt and McMillan[10] (hereafter referred to as BM), Bhatt,[11-13] and Bhatt and Lee[14] to consider generalized Landau theories of the martensitic transition involving direct coupling of the electronic order parameter to the lattice dilatation (as in the Labbé-Friedel model) or coupling due to dimerization of transition-metal atoms (as in

Gorkov's Peierls-gap model). A model calculation by Bhatt[11] for a three-dimensional two-band tight-binding model of the $A15$ compounds exhibited an instability of the electronic spectrum due in part to a Jahn-Teller effect and in part to a Peierls-type gap. This demonstrated the validity (and possible coexistence) of these concepts independent of the one-dimensional models from which they originated.

Subsquently, Bhatt[11] showed that phenomenological Landau theories based on either coupling mechanism take a common phenomenological form with one exception: Only direct coupling between an incipiently unstable charge distribution and the E_g optical phonon (and not indirect coupling via the strain) should produce a softening of that phonon with decreasing temperature. Experimental evidence for such a direct coupling is provided by the observed softening of the E_g phonon in V_3Si (Refs. 15—18) and Nb_3Sn (Ref. 18). The temperature dependence of the peak frequency of the E_g optical phonon, derived in the dynamical Landau theory of BM for the case of direct coupling to a Peierls-type intrachain charge-density distortion, qualitatively reproduces the experimentally observed softening for these two compounds. However, this does not imply that intrachain charge-density distortions are the primary order parameter for the martensitic transition. A qualitatively similar E_g optical-phonon softening would be predicted by a dynamical Landau theory based on a generalized Jahn-Teller model[11] if direct coupling were also included between the E_g optical phonon and intrachain charge-density distortions. Since the essential difference between the models is basically the form of the electron-phonon coupling, the question as to which microscopic (as opposed to phenomenological) model is appropriate depends on details of the band structure near the Fermi surface in these compounds.

In spite of the enormous difficulties in formulating an exact microscopic model of the band structure of the $A15$ compounds, several high-quality *ab initio* band-structure calculations have been performed in recent years.[19—24] Klein, Boyer, and Papaconstantopoulos have done relativistic, self-consistent augmented-plane-wave (APW) calculations for over a dozen $A15$ compounds, including V_3Si, V_3Ge, Nb_3Sn,[19] and Nb_3Sb.[22] In all the compounds studied to date, a common feature is the very flat bands which evolve from the Γ_{12} level and give rise to sharp structure in the density of states. Mattheiss and Weber[25] calculated a highly accurate fit to the APW results for cubic V_3Si and Nb_3Sn using a nonorthogonal—tight-binding (NTB) scheme. This allowed them to show that the small dispersion of the Γ_{12} bands over a large fraction of the Bril-

louin zone is due primarily to strong interchain transition-metal hybridization. The magnitude of the electron-phonon interaction and the superconducting transition temperature T_c can be correlated with the nearness of the Fermi level to these bands.[26] In the high-T_c compounds V_3Si (Ref. 19) and Nb_3Sn,[19,20] the Fermi level slices through these flat bands, remaining within ~ 0.03 eV of them halfway out to the Brillouin-zone boundary along the Δ ($\Gamma—X$), Λ ($\Gamma—R$), and Σ ($\Gamma—M$) directions. For the moderate-T_c (6.3-K) compound V_3Ge,[19] and the low-T_c (0.2-K) compound Nb_3Sb,[22] E_F is placed ~ 0.06 eV and ~ 0.35 eV, respectively, above these very flat bands.

Recently, attention has been focused on the role played by these very flat bands emanating from the Γ_{12} level in driving the martensitic transition. Kataoka[27] has investigated the effect of strain on the Γ_{12} bands (i.e., the bands emanating from the Γ_{12} level). By performing a finite-temperature calculation of the free energy of the electron-lattice system for a simplified model of the Γ_{12} bands coupled to the strain, he was able to quantitatively reproduce the elastic softening in V_3Si and Nb_3Sn. Pickett and co-workers[21] have calculated the effect of chain dimerization on the Γ_{12} level in Nb_3Ge. They find that the Γ_{12} level splits, with the "bonding" (along the chain) state raised above the Fermi level. In addition, they estimate that chain dimerization in Nb_3Sn typically causes energy shifts and splittings at high-symmetry points of ~ 0.04 eV. Weber and Mattheiss[28] have applied the NTB scheme to calculate the electronic structure of tetragonal Nb_3Sn using parameters derived from their earlier NTB analysis of cubic Nb_3Sn.[25] They find a symmetric splitting (~ 0.09 eV) of the cubic Γ_{12} bands in the tetragonal state, about 80% of which is due to dimerization of the Nb sublattice. This dimerization produces a large additional p-d intrachain hybridization. Energy considerations lead them to conclude that splitting of the Γ_{12} bands is the driving mechanism for the tetragonal distortion. These results indicate that both E_g strain and the E_g optical phonon are directly coupled to the charge-density distortions, with coupling to the E_g optical phonon being the dominant interaction.

Since the martensitic transition involves dimerization of the linear chains of transition-metal ions, which is equivalent to a condensation of the optical phonon of E_g (Γ_{12}) symmetry,[29] Raman scattering studies of this phonon in a variety of $A15$ compounds can provide valuable insight as to which microscopic electron-phonon—coupling mechanism is connected with the anomalies in these compounds. Previous Raman scattering studies of this phonon in V_3Si (Refs. 15—18) and Nb_3Sn (Ref. 18) have shown

it to soften with decreasing temperature, to have an asymmetric line shape, and to be strongly damped, with the damping increasing $\sim 100\%$ upon cooling from ~ 400 to ~ 50 K. The linewidth decreased dramatically upon cooling below ~ 80 K in transforming V_3Si,[18] but remained essentially constant in nontransforming Nb_3Sn (Ref. 18) and nontransforming V_3Si (Refs. 15—18). An explanation of this effect in terms of Raman scattering from tetragonal microdomains near the surface in transforming samples has been proposed.[18] Recently work has been completed on V_3Si irradiated with 37-MeV protons (fluence $\phi = 4.6 \times 10^{18}$ cm^{-2}).[16] Irradiation reduced T_c from 16.5 to 6.5 K (Ref. 30) and simultaneously reduced the E_g optical-phonon linewidth $\sim 50\%$. It was conjectured that irradiation produces a homogeneous distribution of defects which reduces the electronic density of states, and hence the electron-phonon coupling, due to a disorder-induced reduction in the electronic mean free path.[16]

In a continuing effort to understand the anomalous temperature-dependent E_g-mode linewidth and the effect on the linewidth of the placement of the Fermi level with respect to the Γ_{12} bands, we have extended our Raman scattering measurements to V_3Ge ($T_c = 6.3$ K) and Nb_3Sb ($T_c = 0.2$ K). These two compounds are of interest for several reasons. First, neither compound exhibits a bulk martensitic transformation, so it is reasonable to assume that the effect of tetragonal microdomains near the surface, if present, on the Raman spectra should be greatly suppressed. Second, the calculated progressive increase in energy separation between the Fermi level and the Γ_{12} bands in going from V_3Si to Nb_3Sn to V_3Ge to Nb_3Sb allows us to systematically study any consequent effect on the E_g phonon in systems with otherwise very similar band structures. Our data on the E_g phonon in V_3Ge show a similar, although weaker, anomaly to that seen in V_3Si and Nb_3Sn. The anomaly is completely absent in Nb_3Sb, however, for which we observed both the E_g and T_{2g} (Γ'_{25}) optical phonons. These phonons in Nb_3Sb behave as expected of phonons whose self-energy is dominated by the usual anharmonic interactions. We have also extended previous measurements on V_3Si,[15] believed to be nontransforming, to several new temperatures down to 30 K. We point out a correlation between magnetic susceptibility and E_g-mode linewidth in V_3Si, Nb_3Sn, and V_3Ge. It is demonstrated by scaling arguments that V_3Si, Nb_3Sn, and V_3Ge exhibit very similar temperature dependences in the E_g phonon linewidth, with the remaining small differences dependent upon details of the distribution of the joint electronic density of states with respect to the

Fermi level. We relate our results to models of the martensitic transformation and to the results of the band-structure calculations by developing a simple model with which most of the features of the Raman scattering data can be understood in terms of direct coupling of the E_g phonon to interband electronic transitions between the very flat bands emanating from the Γ_{12} level. These results, indicating strong direct coupling of the E_g optical phonon to the Γ_{12} bands, provide support for the recent model of the driving mechanism for the tetragonal distortion,[28] which is based on splitting of the cubic Γ_{12} $N(E)$ peak predominantly by the dimerization of the transition-metal sublattice. We conclude with suggestions for more rigorous tests of our simple model of the E_g mode. A brief report of some aspects of this work has already appeared.[31]

II. EXPERIMENTAL DETAILS

A single crystal of V_3Ge was grown from buttons of stoichiometric arc-melted starting material by the Czochralski technique in a tri-arc furnace using a water-cooled hearth in 1 atm of argon.[32] The superconducting transition temperature and width at the seed end of the boule were $T_c = 6.46$ K and $\Delta T_c = 0.12$ K; at the other end $T_c = 6.03$ K and $\Delta T_c = 0.03$ K. The Raman scattering sample was from an intermediate position. A (100) surface was spark cut and then mechanically polished with alumina. The final polishing step utilized 0.05-μm γ-alumina, after which no imperfections were visible on the sample surface under a microscope with a magnification of $45\times$. All of the data reported here on V_3Ge and V_3Si were collected on mechanically polished surfaces. To determine if residual strains introduced by the polishing affected the Raman scattering data, several runs were repeated after an additional electropolish using an aluminum electrode in a solution of two parts of 85% lactic acid and one part each of 48% HF, 70% HNO$_3$, and 95% H$_2$SO$_4$ for 8 min at 6 V. It was determined by weighing the sample before and after electropolishing that this removed a surface layer of ~ 100 μm. Electropolished surfaces are known to be relatively strain free. No significant differences were observed between data taken on the differently prepared surfaces. The data for V_3Si reported here were taken on the same sample that earlier measurements[15] were reported on. Although a conclusive determination of whether or not the sample is martensitically transforming is lacking, it is believed to be nontransforming, as this is typical[33,34] for samples with relatively low residual resistivity ratio (RRR) such as ours (an RRR of 12.5). For the investigation on Nb_3Sb, a large single crystal was grown by closed-

tube vapor transport with iodine as a transporting agent. The purity of the starting material was 0.9999% pure for the Sb and is estimated to be 0.999% pure for the Nb. The Raman measurements on the Nb_3Sb were performed on a high-quality, smooth, as-grown (112) face of the crystal, so that no surface preparation was necessary. Laser light of 514-nm wavelength was incident at a pseudo Brewster angle of 70°; the 0.85-W (V_3Si, V_3Ge) or 0.2-W (Nb_3Sb) beam formed a 2.5×0.13 mm^2 (V_3Si, V_3Ge) or 2.0×0.05 mm^2 (Nb_3Sb) illuminated area. The scattered light was collected in a direction normal to the surface and focused onto the entrance slit of a home-built 1.0-m double monochromator equipped with 2000-lines/mm concave holographic gratings. An RCA C31034-05 photomultiplier tube was used for the detector along with standard photon-counting equipment. The resolution was typically 10 cm^{-1} for the runs on V_3Si and V_3Ge, and 2.0 cm^{-1} for the runs on Nb_3Sb.

For measurements down to 50 K, cooling was provided by flowing cold helium gas in a modified "Heli-Tran" system. A liquid-He Janis cryostat in conjunction with reduced laser power was used for measurements below 50 K. The temperatures quoted for the V_3Si, V_3Ge, and Nb_3Sb data were determined as follows: At a thermocouple temperature of 200 K, the anti-Stokes to Stokes ratio of the E_g phonon was measured to determine the true sample temperature. This established the temperature rise per watt of laser-beam power, and the temperatures of other runs were corrected accordingly. Each time the laser beam was refocused on the surface for a new set of runs, the degree of heating, which was typically 50—100 K/W, was redetermined. This amount of laser-beam heating is in qualitative agree-

TABLE I. Fitting parameters for V_3Ge (cm^{-1}).

Temperature (K)	Ω	E_g phonon Γ (FWHM)	Ω_a
400	280.9	36.9	435
375	281.6	39.4	435
350	282.9	41.4	437
325	281.4	42.9	439
300	282.2	43.6	426
275	283.1	47.8	419
250	282.5	48.2	430
225	283.5	52.4	419
200	284.3	52.7	421
175	286.0	54.7	410
150	287.2	58.1	410
125	288.8	56.8	401
80	286.1	65.7	416
50	287.3	69.6	439

ment with estimates for V_3Si derived from the heat equation, assuming a rectangularly shaped power input to a semi-infinite solid and the thermal conductivity measured by Hegenbarth and Schmidt.[35]

The Raman spectra of V_3Ge at 340 and 50 K taken with a $[(100),(1\bar{1}0)]$ polarization geometry (E_g spectra) are shown in Fig. 1. As in the case of V_3Si and Nb_3Sn, the E_g phonon has three anomalous properties: temperature dependence of peak position and linewidth, and asymmetric line shape. The peak frequency is seen to harden upon cooling for V_3Ge whereas it softens upon cooling for both V_3Si and Nb_3Sn. The solid lines in Fig. 1 are fits to a spectral function resulting from a coupled-mode theory, wherein the asymmetric phonon line shape is due to a Briet-Wigner-Fano interference between the
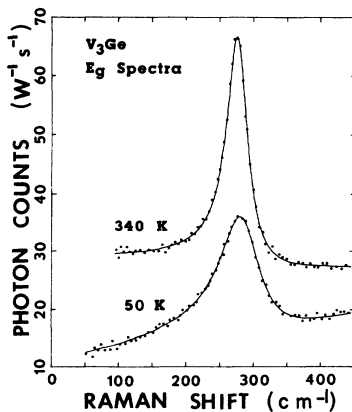

FIG. 1. E_g-symmetry Raman spectra for V_3Ge taken at 340 and 50 K. The data at 340 K have been shifted upward by 20 counts/W s. Lines represent fits to Eqs. (1) and (2): Lorentzian with antiresonance.
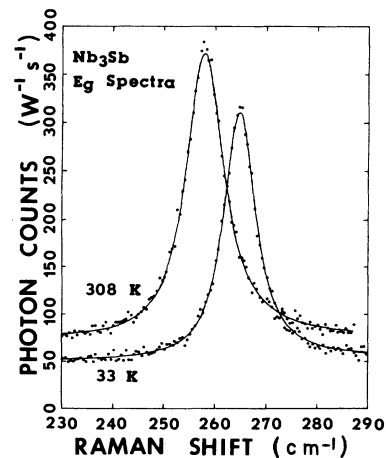

FIG. 2. E_g-symmetry Raman spectra for Nb_3Sb taken at 308 and 33 K. Lines represent fits to simple Lorentzians.
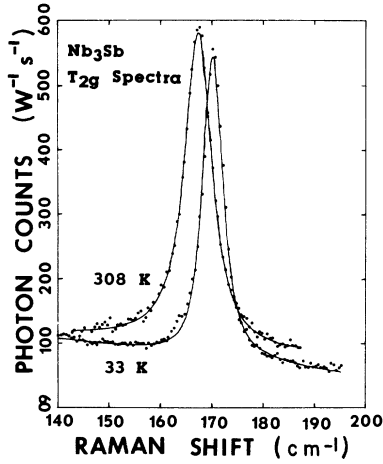
FIG. 3. T_{2g}-symmetry Raman spectra for Nb₃Sb taken at 308 and 33 K. Lines represent fits to simple Lorentzians.

discrete phonon and an electronic continuum,[15,36] namely,

$$S(\omega) = \frac{h\pi^{-1}(1-e^{-\beta\omega})^{-1}2\Gamma\omega\alpha_c^2 f(\omega)}{(\Omega^2-\omega^2)^2+\omega^2\Gamma^2} , \quad (1)$$

$$f(\omega) = (\Omega_a^2-\omega^2)^2/\lambda^2 . \quad (2)$$

The parameters resulting from these fits are given in Table I. Here Ω is the renormalized phonon frequency, Γ is its width [full width at half maximum (FWHM)], Ω_a is the antiresonance frequency, λ is a coupling constant between the phonon and the electronic continuum, and α_c is the amplitude for Raman coupling to the continuum.

Measurements on V₃Ge taken in the polarization geometry that produces T_{2g} spectra revealed very weak scattering from the Raman-active T_{2g} shearing mode, with a peak frequency of 185 cm⁻¹ and a linewidth (FWHM) of ∼26 cm⁻¹ at 300 K. Owing to the very weak scattering from this mode, a com-

plete study of its temperature dependence has not been completed at this time. The T_{2g} mode is not observable in the only other V-based $A15$ compound studied to date, V₃Si, although it is observable in the Nb-based compounds Nb₃Sn and Nb₃Sb, and in the Cr-based compound Cr₃Si.[31,37]

In addition to the E_g mode, Fig. 1 shows the presence of background scattering which linearly increases with increasing frequency shift. The slope of this background increases with decreasing temperature. We believe at least part of this continuum to be electronic Raman scattering (as opposed to luminescence) which interferes with scattering from the E_g phonon, giving the phonon its asymmetric line shape. This background scattering continues to increase with increasing frequency shift, reaching a very broad maximum intensity of several times the E_g phonon intensity at several thousand cm⁻¹ frequency shift. We have observed such scattering for V₃Si, V₃Ge, Nb₃Sn, Nb₃Sb (although it appears much weaker at low frequency shifts in Nb₃Sb), and Cr₃Si, so it appears to be a general property of $A15$ compounds. A detailed study of this feature will be the subject of planned future work.[38]

The E_g- and T_{2g}-symmetry Raman spectra of Nb₃Sb at 308 and 33 K are shown in Figs. 2 and 3, respectively. In contrast to the behavior in V₃Si,[15-18] Nb₃Sn,[18] and V₃Ge, both the E_g and T_{2g} phonons have symmetrical, relatively narrow line shapes, the widths and frequencies becoming even narrower and harder upon cooling. The fits to the data in Figs. 2 and 3 were made with simple Lorentzians superimposed on a linear background. The parameters resulting from these fits are given in Table II. The frequencies of these modes are in good agreement with the values reported in the recent neutron scattering results of Pintschovious et al.[39] The decreasing background with increasing frequency shift evident in the T_{2g} spectra of Fig. 3 is an artifact of the limited ability of the monochromator to reject the intense stray laser light. The ap-

TABLE II. Fitting parameters for Nb₃Sb (cm⁻¹).

Temperature (K)	E_g phonon Ω	Γ (FWHM)	T_{2g} phonon Ω	Γ (FWHM)
308	257.8	8.3	167.2	5.6
283	257.0	8.1	167.4	5.3
258	258.6	8.2	167.4	5.1
208	261.3	8.5	168.5	5.5
158	262.1	7.6	168.2	5.0
133	263.1	7.8	169.0	4.8
108	264.0	7.6	169.9	5.3
83	264.1	7.0	169.6	4.6
58	264.5	6.9	170.1	4.0
33	264.6	6.8	170.2	3.5

parent lack of background scattering which increases with increasing frequency shift in Figs. 2 and 3 results from these runs being taken with relatively high resolution (2.0 cm^{-1}), which decreased our sensitivity to the already weak background.

We also report here the results of an extension of the measurements of Wipf et al.[15] on V$_3$Si to several new temperatures, particularly below 150 K. The results of our fits to these data are given in Table III.

The most prominent feature of the Raman spectra for V$_3$Si,[15,18] Nb$_3$Sn,[18] and V$_3$Ge is the dramatic broadening of the E_g phonon, beginning at temperatures as high as 400 K and reaching a maximum increase of $\sim 100\%$ below 100 K. The temperature dependence of the broadening for V$_3$Si and V$_3$Ge is shown in Fig. 4(a), where the linewidth (FWHM) is plotted versus temperature. In the nontransforming V$_3$Si,[15,18] Nb$_3$Sn,[18] and V$_3$Ge, the linewidth begins broadening at ~ 400 K and reaches a maximum constant value for temperatures below ~ 50 K. In transforming V$_3$Si,[18] the line shape attains a broad maximum at ~ 90 K and then decreases $\sim 35\%$ upon further cooling.

A similar, although weaker, anomaly is seen in the temperature dependence of the E_g-mode frequency, plotted in Fig. 4(b) for V$_3$Si and V$_3$Ge. For nontransforming V$_3$Si (Refs. 15 and 18) the frequency begins decreasing at ~ 400 K and reaches a constant minimum value for temperatures below ~ 120 K. In both transforming V$_3$Si (Ref. 18) and nontransforming Nb$_3$Sn (Ref. 18), however, the frequency decreases upon cooling below ~ 400 K, reaches a
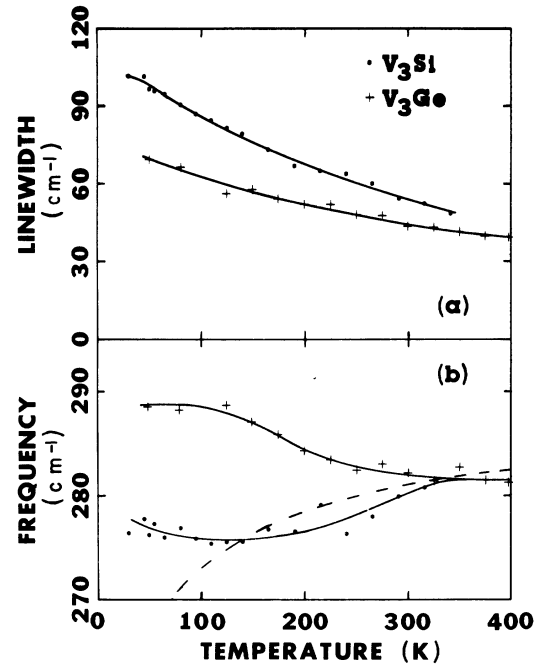

FIG. 4. Temperature dependence of the linewidth (FWHM) (a) and frequency (b) of the E_g mode for V$_3$Si and V$_3$Ge. Solid curves serve as a guide to the eye. Dashed curve is theoretical frequency dependence calculated from theory of Ref. 10 assuming values for their parameters of $R=2.1$, $\omega_0=287$ cm^{-1}, and $T_m=20$ K.

minimum at ~ 120 and ~ 90 K and then increases upon further cooling. This softening is precisely what was predicted in BM for direct coupling between the E_g optical phonon and the electric instability. An opposite behavior is observed in V$_3$Ge, where the E_g frequency is seen to harden slightly upon cooling, reaching a constant maximum value for temperatures below ~ 125 K.

It should be pointed out that all of the frequencies and linewidths reported here for nontransforming V$_3$Si (and in Ref. 15) and for V$_3$Ge were obtained by fitting the data with asymmetric line-shape functions as discussed in Ref. 15. Schicktanz et al.[18] do not explicitly state in their study of transforming and nontransforming V$_3$Si and nontransforming Nb$_3$Sn what fitting procedure they followed, but we assume from their discussion[18] that they fitted their data with symmetric line-shape functions. Thus there may be a systematic discrepancy between the fitting parameters reported for the two groups of compounds.

III. DISCUSSION

A. Landau theories for the E_g optical phonon

The spectral function for one-phonon Stokes Raman scattering is given by the generalized

TABLE III. Fitting parameters for V$_3$Si (cm^{-1}).

Temperature (K)	Ω	E_g phonon Γ (FWHM)	Ω_a
340	281.4	47.5	451
315	280.7	51.7	443
290	279.9	53.4	445
265	278.0	59.4	455
240	276.3	63.6	463
215	279.1	64.6	457
190	276.5	66.6	453
165	276.7	73.0	447
140	275.5	79.4	445
125	275.6	81.5	443
110	275.4	84.6	444
95	275.8	87.1	437
80	276.9	90.4	432
65	276.0	94.7	439
60	277.4	96.0	459
52	276.2	96.6	438
45	277.9	101.5	489
30	276.4	101.2	500

fluctuation-dissipation theorem to be

$$S(\vec{q},\omega)=\hbar\pi^{-1}[1+n(\omega)]\mathrm{Im}D(\vec{q},\omega) , \tag{3}$$

where $[1 + n(\omega)]$ is the usual thermal factor for bosons and $D(\vec{q},\omega)$ is the one-phonon Green's function. In the presence of electron-phonon interactions, $D(\vec{q},\omega)$ is obtained using Dyson's equation

$$D^{-1}(\vec{q},\omega)=D_0^{-1}(\vec{q},\omega)-\Pi(\vec{q},\omega) , \tag{4}$$

where

$$D_0(\vec{q},\omega)=\frac{\omega_0(\vec{q})}{\omega^2-\omega_0^2(\vec{q})} \tag{5}$$

is the noninteracting phonon Green's function and

$$\Pi(\vec{q},\omega)=\sum_{\vec{k},n,n'} \langle\,|M_{\vec{k},n;\vec{k}+\vec{q},n'}|\,\rangle^2$$

$$\times X_{\vec{k},n,n'}(\vec{q},\omega) \tag{6}$$

is the phonon self-energy. Here $\vec{k}$ is an electronic wave vector, n and n' are band indices, $\langle\,|M_{\vec{k},n;\vec{k}+\vec{q},n}|\,\rangle^2$ is the square of an electron-phonon matrix element, and $X_{\vec{k},n,n'}(\vec{q},\omega)$ is the electronic susceptibility. Π can be written more explicitly as

$$\Pi(\vec{q},\omega)=\sum_{\vec{k},n,n'} \langle\,|M_{\vec{k},n;\vec{k}+\vec{q},n'}|\,\rangle^2[f(E_{\vec{k},n})-f(E_{\vec{k}+\vec{q},n'})]\mathscr{P}\,\frac{1}{E_{\vec{k},n}-E_{\vec{k}+\vec{q},n'}+\omega}$$

$$-i\pi\sum_{\vec{k},n,n'} \langle\,|M_{\vec{k}n;\vec{k}+\vec{q},n'}|\,\rangle^2[f(E_{\vec{k},n})-f(E_{\vec{k}+\vec{q},n'})]\delta(\omega-E_{\vec{k}+\vec{q},n'}+E_{\vec{k},n}) , \tag{7}$$

where $f(E_{\vec{k},n})$ is a Fermi factor and the symbol $\mathscr{P}$ denotes the principal value.

Shirane and Axe[40] were able to explain the central peak which they observed in their neutron scattering study of Nb$_3$Sn by including Akhiezer loss effects[41,42] due to linear coupling of the acoustic modes to pairs of thermal phonons. This can be modeled by a phenomenological expression for the phonon self-energy:

$$\Pi=\frac{\delta}{1-i\omega\tau} , \tag{8}$$

where τ is the relaxation time of the thermal phonons and δ is proportional to the third-order anharmonic coupling coefficient. This form for Π leads to a three-peaked spectral function in agreement with their data, although a detailed comparison of the values of δ and τ to those expected for Nb$_3$Sn was not attempted.

More generally, a phonon self-energy of the form (8) can result from linear coupling of the phonon to any fluctuations characterized by a Debye-type relaxation mechanism. In those metals in which heat is transported primarily by the electrons, electron-phonon coupling to a relaxing electron distribution usually dominates over Akhiezer effects.[42] In this case, δ is proportional to the strength of the electron-phonon interaction and τ is a collective electronic relaxation time. This is the spirit in which the various Landau theories have been formulated in attempting to account for the anomalous ultrasonic absorption[43-45] and the central peak observed in neutron scattering studies.[40]

The Landau theory of BM (Ref. 10) is equivalent to assuming

$$\Pi(\vec{q},\omega)=g^2\frac{X_0}{1-i\omega\tau} , \tag{9}$$

where, as usual in a Landau theory, the static density response function X_0 is taken to have the form

$$(X_0)^{-1}=a(T-T_m) , \tag{10}$$

where T_m is the martensitic transition temperature. The source of the temperature dependence in (9) is thought to be the Fermi factors in (7). As shown in BM, this leads to a three-peaked spectral function for both the acoustical and optical phonons characterized by asymmetric phonon line shapes, decreasing phonon frequencies, and increasing phonon linewidths as the temperature is reduced. This is due to critical slowing down of the electron distribution as T_m is approached. The electrons then no longer adiabatically follow ionic motion, resulting in a softer, more damped phonon.

It is tempting to ascribe the anomalous characteristics of the E_g optical phonon to this mechanism. For $T > T_m$, the theory of BM predicts an optic-phonon linewidth which increases with decreasing temperatures as $1/(T-T_m)$, in qualitative agreement with experiment. Increasing the electronic dissipation increases the magnitude of the linewidth and, for large enough dissipation, results in a central peak at low temperatures. However, the experimentally observed absence of the "forbidden" (300) reflection in Nb$_3$Sn (Ref. 40) and the absence of any trace of a central peak in the Raman scattering data on V$_3$Si (Refs. 15-18) and Nb$_3$Sn (Ref. 18)

place an experimental upper bound on the electronic dissipation. This results in *upper*-bound estimates for the linewidth and degree of asymmetry at least a factor of 3 too small to explain the experimental data. It is concluded in BM that the central peak seen in neutron scattering[40] and the anomalous ultrasonic absorption[43–45] are also not ascribable solely to electron dynamics. The former is in agreement with either impurity scattering[10] or Akhiezer loss,[40] and the latter has been attributed to domain-wall reorientation and domain-boundary scattering of acoustic waves.[43–45] Thus the majority of experimental data indicate that although electronic relaxation effects may make a small contribution to the lattice dynamics of $A15$ compounds undergoing a martensitic transition, a different mechanism is needed to explain the anomalous characteristics of the E_g optical phonon.

B. Experimental correlation of magnetic susceptibility with E_g phonon linewidth

The temperature dependence of the linewidth displayed in Fig. 4(a) is very reminiscent of that of the magnetic susceptibility χ. The magnetic susceptibility has been measured in both transforming[33,34,46,47] and nontransforming[33,34,46–48] V_3Si, and in transforming Nb_3Sn,[49] V_3Ge,[48] and Nb_3Sb.[50] In transforming V_3Si (Refs. 33, 34, 46, and 47) and Nb_3Sn (Ref. 49), χ begins increasing upon cooling below $\sim$400 K, reaching a maximum increase of $\sim$60% at the martensitic transition temperature T_m in V_3Si, and of $\sim$300% at $T_m + 10$ K in Nb_3Sn; it then decreases $\sim$11% and $\sim$6%, respectively, upon further cooling. There are also anomalous features in χ for transforming V_3Si at temperatures as high as 90 K.[33] In nontransforming V_3Si (Refs. 33, 34, and 46–48) and V_3Ge (Ref. 47) the peak in χ disappears and one observes only an increase to a constant maximum increase of $\sim$50% and $\sim$21%, respectively, upon cooling. χ for Nb_3Sb,[50] on the other hand, has a magnitude of only $\sim$40% and $\sim$15% of χ for Nb_3Sn and V_3Si, respectively, at 300 K and increases upon cooling only $\sim$7%. The striking similarity in the temperature-dependent behavior of the E_g-mode linewidth and the magnetic susceptibility in V_3Si, Nb_3Sn, and V_3Ge is further demonstrated by plotting χ versus the corresponding E_g-mode linewidth at the same temperature, for various temperatures. This is shown in Fig. 5, where a strong correlation is seen to exist, with the V-based compounds following one relationship and Nb_3Sn a separate one. The temperature dependence of the magnetic susceptibility is commonly ascribed to thermal repopulation of electronic energy levels near a sharp peak in the electronic density of states.
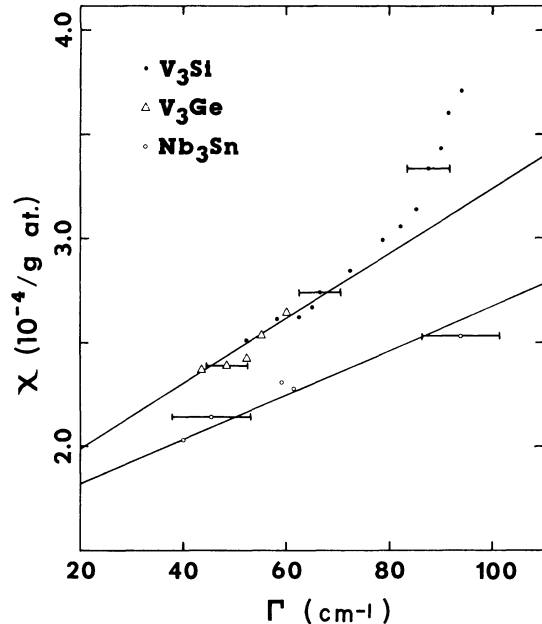

FIG. 5. Magnetic susceptibility χ vs the corresponding E_g-mode linewidth Γ at the same temperature, for various temperatures for V_3Si, V_3Ge, and Nb_3Sn. Raman scattering data for Nb_3Sn taken from Ref. 18. χ data for V_3Si, V_3Ge, and Nb_3Sn taken from Refs. 47 and 48.

The strong correlation between χ and the phonon linewidth Γ, shown in Fig. 5, suggests that electron-phonon interactions (as opposed to anharmonic phonon-phonon interactions), subject to the same thermal repopulation effects as χ, are responsible for the temperature dependence of Γ and Ω of the E_g phonon in these compounds. Such a strong correlation is initially surprising, since χ is essentially the thermally averaged single-electron density of states while Γ is a different thermal average of the joint electronic density of states. However, we show below that these two expressions have approximately identical temperature dependences for $T/\Omega \gtrsim \frac{1}{4}$ within the context of our model for the linewidth.

C. Asymmetry of E_g phonon line shape

Inspection of the energy-band calculations of Klein *et al.*[19] reveals that the flat bands emanating from the Γ_{12} level are apparently separated by an energy comparable to the E_g phonon energy over large regions of $\vec{k}$ space. We propose that the dominant damping mechanism for the E_g mode consists of interband processes wherein the E_g mode decays into electron-hole pairs in these bands. Symmetry constraints place certain selection rules on the matrix elements for such processes. It is easily shown that coupling to interband excitations involving electronic states along the Δ, Σ, and Λ directions in $\vec{k}$

space is allowed for the E_g mode and not allowed for the T_{2g} mode. These selection rules are expected to extend with little modification to arbitrary k near the Γ point and these lines as well. It is understandable, then, that the T_{2g} mode is damped much more weakly (FWHM ~ 10 cm^{-1}) than the E_g mode (FWHM ~ 40 cm^{-1}) in Nb₃Sn at room temperature.[18]

In general, one may also expect to observe a continuum of interband electronic Raman scattering between these same bands. This will interfere with the one-phonon Raman scattering, resulting in an asymmetric line shape similar to that seen in studies of degenerate p-type silicon.[51] The theoretical description of this phenomena has been treated by many authors and reviewed by Klein.[36] The result for the spectral function of the optical phonon is a Lorentzian with a superimposed Fano-type antiresonance, i.e., Eqs. (1) and (2). As stated earlier, we believe that the linearly increasing background observed in Raman scattering from $A15$ compounds represents a continuum of interband electronic Raman scattering and that the asymmetry of the phonon line shape results from interference with this continuum. The interference need not be complete; the intensity at Ω_a need not be zero.[36]

The data display only a weak asymmetry, however, and as a result there is a scatter of $\sim \pm 5\%$ in the antiresonance frequencies listed in Tables I and III, the curves of the fit not being very sensitive to small changes in Ω_a. Similarly, the broad phonon line shapes render the fits less sensitive to small changes in the phonon frequency. These difficulties along with the usual signal-to-noise problems encountered in Raman scattering studies of metals account for the small amount of scatter in the values of Ω and Ω_a listed in Tables I and III. A similar degree of scatter would exist were the data to be fitted with some other function. Nevertheless, the fits using the antiresonance formula (1) and (2) have significantly smaller mean-square deviations than fits based on a simple Lorentzian line shape.[15] In addition, the general trends are clear, with Ω_a decreasing upon cooling to ~ 90 K and then increasing upon further cooling in both V₃Si and V₃Ge. No attempt has yet been made to relate Ω_a to microscopic band-structure parameters.

D. Temperature dependence of the E_g phonon linewidth

Now we will show how, on the basis of a simple model, decay of the E_g optical phonon into electron-hole pairs in the Γ_{12} bands can explain the observed temperature dependence of the linewidth. These electron-phonon interaction processes cause

the phonon to acquire a complex self-energy, the real part giving the phonon-frequency renormalization and the imaginary part giving the phonon linewidth. The imaginary part of the phonon self-energy [Eqs. (6) and (7)] can be written in condensed form as the product of an electron-phonon coupling constant squared and the imaginary part of an electronic response function:

$$\mathrm{Im}\Pi(\omega) = \lambda^2 \mathrm{Im}\mathcal{X}(\omega) \ . \tag{11}$$

As the imaginary part of a response function, $\mathrm{Im}\mathcal{X}(\omega)$ must be an odd function of ω. We make the simple assumption

$$\lambda^2 \mathrm{Im}\mathcal{X}(\omega) = \Gamma\omega \ , \tag{12}$$

where Γ is the (frequency-independent) phonon linewidth. Combining Eqs. (4), (5), (7), (11), and (12) and including interference effects[15,36] results in Eqs. (1) and (2) for $S(\omega)$, where the phonon linewidth is given by

$$\Gamma \frac{\pi}{\Omega_Q} \sum_{\vec{k}} \langle\, |M_{\vec{k},n;\vec{k}+\vec{Q},n'}|\,\rangle^2$$

$$\times [f(E_{\vec{k},n}) - f(E_{\vec{k}+\vec{Q},n'})]$$

$$\times \delta(\Omega_{\vec{Q}} - E_{\vec{k}+\vec{Q},n'} + E_{\vec{k},n}) \tag{13}$$

and $\langle\, |M_{\vec{k},n;\vec{k}+\vec{Q},n'}|\,\rangle$ is the matrix element for scattering from an electron state $\vec{k}$ in band n of energy $E_{\vec{k}n}$ to a state $\vec{k}+\vec{Q}$ in band n' of energy $E_{\vec{k}+\vec{Q},n'}$ via a phonon of wave vector $\vec{Q}$ and energy $\Omega_{\vec{Q}}$. Since we are considering a zone-center phonon, we take $\vec{Q}=0$ and define $\Omega_{\vec{Q}}=\Omega$; however, one would expect such processes to be active for phonons well into the Brillouin zone due to the flatness of the Γ_{12} bands. The matrix element $\langle\, |M_{\vec{k},n;\vec{k},n'}|\,\rangle$ includes many-body corrections such as screening, vertex corrections, etc. For our purposes we take it to be constant in temperature and nearly independent of the electronic wave vector $\vec{k}$ and pull it out of the summation. The linewidth temperature dependence is then determined by the Fermi factors $f-f'$. Evaluation of Eq. (13) still involves extensive calculations requiring knowledge of the exact electronic energy levels and the Fermi energy as a function of temperature. In order to facilitate comparison with experiment we make some simplifying assumptions which we expect to yield qualitatively correct results. We consider only the bands n and n' emanating from the Γ_{12} level and measure the electronic energies with respect to the Fermi energy (which we take to be temperature independent). Rewriting (13) in terms of the new variables,
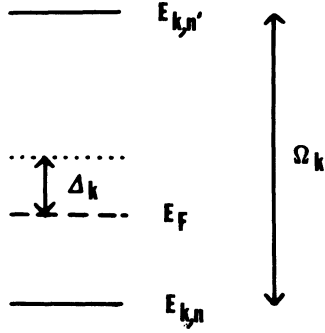
FIG. 6. Relative positions of the arbitrary states $\vec{k},n$ and $\vec{k},n'$ with respect to the Fermi level in terms of $\Omega_{\vec{k}}$ and $\Delta_{\vec{k}}$.

$$\Delta_{\vec{k}}=(E_{\vec{k},n'}+E_{\vec{k},n})/2 , \tag{14a}$$

$$\Omega_{\vec{k}}=(E_{\vec{k},n'}-E_{\vec{k},n}) , \tag{14b}$$

which are illustrated in Fig. 6, gives

$$\Gamma=\frac{\pi}{\Omega}\langle\,|M_{nn'}|\,\rangle^2$$

$$\times\sum_{\vec{k}}\left[f\left[\Delta_{\vec{k}}-\frac{\Omega_{\vec{k}}}{2}\right]-f\left[\Delta_{\vec{k}}+\frac{\Omega_{\vec{k}}}{2}\right]\right]$$

$$\times\delta(\Omega-\Omega_{\vec{k}}) , \tag{15}$$

where $\langle\,|M_{nn'}|\,\rangle^2$ is an average ($\vec{k}$-independent) electron-phonon matrix element squared. This expression tells us that only those pairs of states $\vec{k},n$ and $\vec{k},n'$ whose energies differ by Ω can contribute to the damping of the phonon (as expected simply from energy conservation), and also that the relative position of these pairs of states with respect to the Fermi level $\Delta_{\vec{k}}$ influences the temperature dependence of the damping. We neglect lifetime broadening of the electronic energy levels. Now as the bands n and n' evolve from the Γ_{12} level, the APW band-structure calculations[19] indicate that there are many pairs of states $\vec{k},n$ and $\vec{k},n'$ throughout the Brillouin zone for which $\Omega_{\vec{k}}$ is comparable to the E_g phonon energy and that the "center of gravity" of these states, $\Delta_{\vec{k}}$, is distributed in some narrow region about the Fermi energy. This distribution is just the joint electronic density of states for the bands n and n', $J(E,E+\Omega)$, which we chose to write as $J_\Omega(\Delta)$ (assumed to be temperature independent). The summation over $\vec{k}$ in (15) can thus be converted to an integral over Δ,

$$\Gamma=\frac{\pi}{\Omega}\langle\,|M_{nn'}|\,\rangle^2\int_{-\infty}^{\infty}J_\Omega(\Delta)[f(\Delta-\Omega/2)$$

$$-f(\Delta+\Omega/2)]d\Delta . \tag{16}$$

In order to proceed further, we must assume a form for $J_\Omega(\Delta)$. In keeping with the required oddness of the function $\mathrm{Im}\mathcal{X}(\omega)$, we assume $J_\Omega(\Delta)$ to be a linear function of Ω (at least for Ω on the order of the E_g phonon energy). In view of the narrowness of the Γ_{12} bands[19] we also assume $J_\Omega(\Delta)$ to be a Lorentzian function of Δ of full width $2b$ centered at Δ_0:

$$J_\Omega(\Delta)=\Omega\frac{N_0 b/\pi}{b^2+(\Delta-\Delta_0)^2} \tag{17a}$$

$$\equiv\Omega N_0 j(\Delta) . \tag{17b}$$

Then the linewidth becomes

$$\Gamma=\pi\langle\,|M_{nn'}|\,\rangle^2 N_0^*$$

$$\times\frac{\int_{-\infty}^{\infty}j(\Delta)[f(\Delta-\Omega/2)-f(\Delta+\Omega/2)]d\Delta}{\int_{-\Omega/2}^{+\Omega/2}j(\Delta)d\Delta} \tag{18}$$

or

$$\Gamma=\Gamma_0 F(T/\Omega,b/\Omega,\Delta_0/\Omega) , \tag{19}$$

where $\Gamma_0=\pi\langle\,|M_{nn'}|\,\rangle^2 N_0^*$ is the $T=0$ linewidth, N_0^* is the effective joint density of states at $T=0$,

$$N_0^*=N_0\int_{-\Omega/2}^{+\Omega/2}j(\Delta)d\Delta$$

$$=\frac{N_0}{\pi}\left[\tan^{-1}\left[\frac{\Omega/2-\Delta_0}{b}\right]\right.$$

$$\left.-\tan^{-1}\left[\frac{-\Omega/2-\Delta_0}{b}\right]\right] , \tag{20}$$

and $F(T/\Omega,b/\Omega,\Delta_0/\Delta)$ contains the temperature dependence of the linewidth and is normalized to 1 at $T=0$.

Equation (19) suggests that the reduced linewidths Γ/Γ_0 should all lie on a single curve when plotted versus reduced temperature if the parameters b/Ω and Δ_0/Ω are not too different for the different compounds. This scaling argument is seen to be valid in Fig. 7 where Γ/Γ_0 is plotted versus T/Ω for V_3Si, V_3Ge, and Nb_3Sn. The solid lines through the data are the predicted temperature dependences calculated from a least-squares fit of Eq. (19) to the data. We do not believe the parameters of these fits,
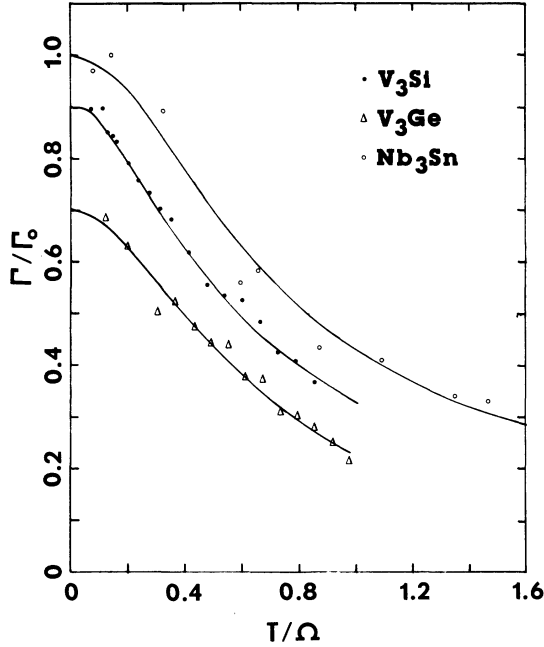
FIG. 7. Reduced linewidth Γ/Γ_0 vs reduced temperature T/Ω, where Ω is the average E_g phonon frequency of each compound, for V$_3$Si, V$_3$Ge, and Nb$_3$Sn. Data for Nb$_3$Sn taken from Ref. 18. The solid curves drawn through the data were calculated with Eqs. (16)—(18) as described in the text. The parameters resulting from these fits are given in Table IV. For clarity, the lower two curves have been shifted down by 0.1 and 0.3, respectively.
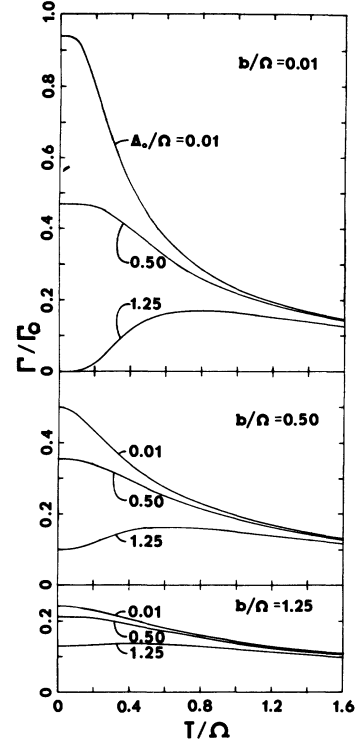

FIG. 8. Reduced linewidth Γ/Γ_0 vs reduced temperature T/Ω calculated from Eqs. (16)—(18) (but not normalized to 1 at $T=0$) showing the effect of variation of the reduced joint electronic density-of-states bandwidth b/Ω, and reduced average energy separation from the Fermi energy Δ_0/Ω.

listed in Table IV, should be taken too literally as describing $J_\Omega(\Delta)$ since, as shown in Figs. 7 and 8, the computed curves are not highly sensitive to the precise values of b/Ω and Δ_0/Ω. In fact, we have obtained similar curves to those shown in Figs. 7 and 8 by modeling $J_\Omega(\Delta)$ as a constant times Ω for Δ within $\pm\Delta_0$ of the Fermi level and equal to zero elsewhere. This is similar to the experience found by other authors in fitting the temperature dependence of the magnetic susceptibility.[34,48,49] However, the qualitative implication of this analysis, i.e., that there exists structure in the joint density of electronic states on the scale of several hundred kelvins, and that this structure is capable of explaining the optic-phonon linewidth, seems clear. Indeed the agreement between theory and experiment in Fig. 7

TABLE IV. Fitting parameters for $J_\Omega(\Delta)$ (cm^{-1}).

	Ω	b	Δ_0
V$_3$Si	277	175.6	0.0
V$_3$Ge	284	267.9	0.0
Nb$_3$Sn	175	22.4	84.7

is remarkable in view of the crudeness of our model of the band structure and our neglect of anharmonic processes. For instance, anharmonic decays to two phonons of frequency $(\Omega/2)$ should contribute a term to the linewidth proportional to $[1 + n(\Omega/2)]^2$, where $n(\Omega/2)$ is a Bose-Einstein factor.

The results for transforming V$_3$Si (Ref. 18) (not plotted) would deviate from the curves in Fig. 7 at low temperatures since the martensitic transformation is known from magnetic susceptibility measurements[33,34,46,47] to reduce the density of states at the Fermi level and to split the Γ_{12} bands.[21,28] We note that this behavior is not inconsistent with (and also not reliant upon) the idea that d-spacing fluctuations[52] in the form of tetragonal microdomains contribute to the linewidth and frequency.[18] The effect of a tetragonal strain and the accompanying dimerizations would be to shift and split the Γ_{12} bands and thus decrease the number of electronic states available for scattering. Thus d-spacing fluctuations enhanced near the surface in A15 compounds with at least a strong tendency to undergo a bulk martensitic transformation could enhance the reduction in

the E_g-mode linewidth, as determined by the surface-sensitive Raman probe, at lower temperatures. The fact that the linewidth begins to decrease at ~ 100 K in the transforming samples[18] suggests that precursive linewidth effects become important well above T_m, similar to the magnetic susceptibility anomalies in the same temperature range.[33] However, the fact that Raman scattering data from $A15$ compounds collected on either mechanically polished or electropolished surfaces and from non-transforming V_3Ge all display an anomalous increase in linewidth upon cooling from temperatures as high as 400 K leads us to discount the suggestion of Schicktanz et al.[18] that the superposition of two peaks, one from cubic and one from tetragonal regions, is the cause of the anomalous broadening. We prefer our explanation in terms of thermal repopulation of electronic energy levels which participate in scattering of the E_g phonon. Conclusive settlement of this question regarding the precursive existence of tetragonal microdomains and their effect on the lattice dynamics will require x-ray studies of the same specimens that the Raman scattering studies are conducted upon. It is perhaps premature to further address this issue until such additional experimental studies become available.

E. Explanation for correlation of χ and Γ

We are now in a position to further understand the correlation between χ and Γ demonstrated in Fig. 5. The measured susceptibility can be expressed as a sum of spin, orbital, and diamagnetic core contributions. The dominant contribution to the temperature dependence of χ has been attributed to the Pauli d-band spin susceptibility. Neglecting exchange effects, this may be written[33] as

$$\chi_d(T) = +\mu_B^2 \int_{-\infty}^{\infty} \left[-\frac{\partial f}{\partial E} \right] N_d(E)dE, \qquad (21)$$

where μ_B is the Bohr magneton and $N_d(E)$ is the d-electron density of states. The experimental χ data have been successfully fit by assuming structure in $N_d(E)$ on the scale of several hundred kelvins. For example, in Ref. 34 excellent agreement with experiment was obtained by taking a Lorentzian distribution for $N_d(E)$, just as we assumed for $J_\Omega(\Delta)$ in explaining the Raman linewidth. The difference between $\chi_d(T)$ and $\Gamma(T)$ thus lies in the replacement of $[f(E-\Omega/2)-f(E+\Omega/2)]$ in $\Gamma(T)$ with $-\partial f/\partial E$ in $\chi_d(T)$. At high temperatures we may expand $[f(E-\Omega/2)-f(E+\Omega/2)]$ to give

$$[f(E-\Omega/2)-f(E+\Omega/2)]$$

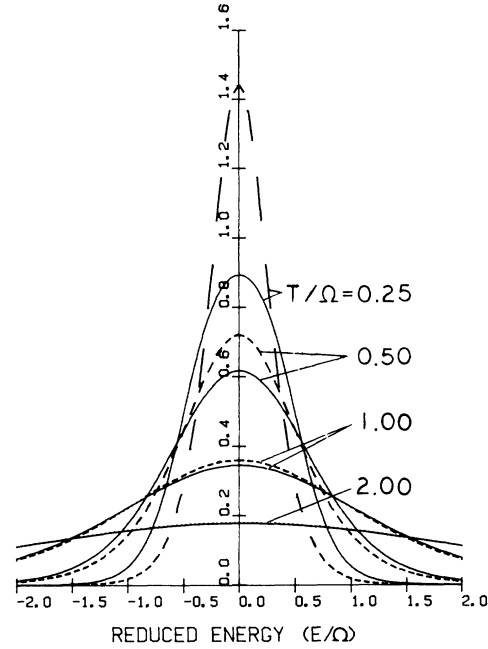$$\simeq -\Omega \, \partial f/\partial E \quad (T \ll \Omega) . \qquad (22)$$

FIG. 9. $-\Omega \, \partial f/\partial E$ (dashed curves) and $[f(E-\Omega/2)-f(E+\Omega/2)]$ (solid curves) vs reduced energy E/Ω for various values of T/Ω.

In Fig. 9 we have plotted $-\Omega \, \partial f/\partial E$ and $[f(E-\Omega/2)-f(E+\Omega/2)]$ vs E/Ω for various values of T/Ω. The two distributions are nearly identical for $T/\Omega \gtrsim \frac{1}{4}$, i.e., for $T \geq 100$ K for V_3Si and $T \geq 65$ K for Nb$_3$Sn. For $T/\Omega \lesssim \frac{1}{4}$, $\chi_d(T)$ is predicted to increase faster than $\Gamma(T)$ with decreasing temperature. This is in qualitative agreement with the results of Fig. 5, where a linear correlation is observed for $T/\Omega \gtrsim \frac{1}{4}$. Of course, a more careful analysis must include the effect of slight differences in $J_\Omega(\Delta)$ and $N_d(E)$ from sample to sample and χ and Γ should both be measured on the same sample. For example, the fact that Γ for the transforming V_3Si samples[18] has a stronger T dependence than Γ for the nontransforming V_3Si samples[15,18] implies a smaller width for $J_\Omega(\Delta)$ in transforming samples. Similarly, measurements of χ show a stronger dependence on T in transforming than nontransforming V_3Si samples.[33,34,46-49] It is expected that when both χ and Γ are measured on the same sample, the correlation demonstrated in Fig. 5 will be obeyed. Thus in the example cited above, Γ for transforming V_3Si (Ref. 18) is expected to fall on the line (for $T/\Omega \gtrsim \frac{1}{4}$) for vanadium-based compounds when plotted against χ measured on that same sample.

Klein et al.[26] have already pointed out the division of V-based and Nb-based $A15$ compounds into two families, with $\eta_{Nb_3B} > \eta_{V_3B}$, where

$\eta = N(E_F)\langle I \rangle^2$, $\langle I \rangle^2$ being a Fermi-surface—averaged electron-phonon matrix element squared. Since $\mathcal{X}$ essentially mirrors changes with temperature of the effective density of states while Γ essentially reflects changes in η, the high-temperature slopes of the two curves, denoted α_V and α_{Nb} for the V-based and Nb-based A15's, respectively, are expected to differ by the ratio of [from Eqs. (18) and (20)]

$$\frac{\alpha_V}{\alpha_{Nb}} \simeq \frac{\langle |M_{nn'}| \rangle_V^2}{\langle |M_{nn'}| \rangle_{Nb}^2} \frac{[N_0^*(E_F)]_V}{[N_0^*(E_F)]_{Nb}} \frac{[N_d(E_F)]_{Nb}}{[N_d(E_F)]_V} .$$

(23)

If we assume that $N_0^*(E_F)$ is proportional to $N_d(E_F)$ with the same value proportionally constant for both V-based and Nb-based compounds and also that $\langle |M_{nn'}| \rangle^2$ is proportional to $\langle I \rangle^2$ with the same value proportionally constant in both compounds, then the ratio of the slopes is just expected to be the ratio of $\langle I \rangle^2$ in the two compounds. Indeed, we find the ratio of the high-temperature slopes of the two curves (indicated by the solid lines through the data in Fig. 5) to be 1.47, in good agreement with the ratio of $\langle I \rangle_{V_3B}^2/\langle I \rangle_{Nb_3B}^2$ of 1.48 as calculated by Klein et al.[26]

Further confirmation of our model is found in comparing the ratios $\Gamma_0^{Nb_3Sn}/\Gamma_0^{V_3Si}$ and $\Gamma_0^{V_3Ge}/\Gamma_0^{V_3Si}$ to the ratios $\eta^{Nb_3Sn}/\eta^{V_3Si}$ and $\eta^{V_3Ge}/\eta^{V_3Si}$, as calculated by Klein et al.[26] Subject to the same provisos regarding proportionalities stated above, we would expect these ratios to be very similar. We find Γ_0 ratios of 0.95 and 0.69, respectively, in good agreement with the calculated η ratios[26] of 0.95 and 0.57.

F. Temperature dependence of the E_g phonon frequency

Turning our attention to the temperature dependence of the frequency of the E_g optical phonon, we note that this can in principle be calculated starting with the real part of the phonon self-energy Π, given in Eq. (7). However, analysis along lines similar to those we have followed in our model for $\Gamma(T)$ would require knowing $J_\Omega(\Delta)$ for all Ω including values of Ω much larger than the E_g phonon energy, where our linear approximation in Eqs. (12) and (17) is less likely to be valid. It is not clear how to model this phenomenologically. Fortunately, even though the dynamical Landau theory of BM (Ref. 10) does not properly account for damping of the E_g optical phonon, it is expected to give qualitatively correct predictions for the temperature dependence of the energy of this mode. The dashed curve through the data for the frequency of the E_g mode of V_3Si in Fig. 4(b)

was calculated from the formula given in BM for a value of their parameter R equal to 2.1 and ω_0 equal to 287 cm^{-1}. The fact that the prediction falls faster with decreasing temperature than the data at low temperatures may be due to the fact that they used the static electronic susceptibility rather than the electronic susceptibility evaluated at the phonon frequency as indicated in Eq. (7) in their calculation. Use of the latter may be expected to soften the temperature dependence at lower temperatures just as Γ exhibits a weaker T dependence than $\mathcal{X}$ at lower temperatures. Furthermore, anharmonic interactions are expected to lead to a hardening of the E_g mode with decreasing temperature, in competition with the softening due to interaction with the CDW. Since V_3Ge does not exhibit a martensitic transition, the contribution due to the CDW is expected to be suppressed relative to the anharmonic contribution in this compound. This can qualitatively explain the observed hardening of the E_g mode of V_3Ge displayed in Fig. 4(b).

In a paper previous to that of BM,[10] Noolandi and Sham[5] have presented a theory of the martensitic transformation in Nb_3Sn using a one-dimensional model for the d electrons (chain model). Their theory allows a calculation of the temperature dependence of the E_g phonon frequency from a fit of suitable parameters to measured elastic constants and tetragonal distortions. With the use of a constant electronic density of states, they predicted well the measured E_g frequency for Nb_3Sn at 200 K (Ref. 18) (years before it was measured), and their paper implicitly allows a calculation of $\Omega(T)$, which agrees reasonably well with the experiment.[53] The model is insufficiently developed to make predictions of the linewidth of this mode.

G. E_g and T_{2g} phonons in Nb_3Sb

The hardening and narrowing of the E_g and T_{2g} phonons in Nb_3Sb upon cooling is typical behavior for phonons whose self-energy is dominated by anharmonic phonon-phonon interactions. This result is consistent with our model since the 0.033-eV E_g phonon cannot interact with the filled Γ_{12} bands ~ 0.35 eV (Ref. 22) below the Fermi level. Furthermore, since the E_g mode only involves motion of the Nb atoms, mass consideration alone would predict it to have essentially the same frequency as in Nb_3Sn (Ref. 18) (~ 170 cm^{-1}). The fact that the frequency is much greater in Nb_3Sb (~ 260 cm^{-1}) is expected since the degree of frequency renormalization due to the electron-phonon interaction is much smaller in Nb_3Sb. In fact, the E_g-mode frequency of Nb_3Sb is probably indicative of the "bare" E_g-mode frequency of Nb_3Sn before frequency renormalization. The

total lack of asymmetry in the E_g and T_{2g} phonon line shapes and the relative weakness of the linear background in Nb$_3$Sb are also what we would expect when the Fermi level is so far above the Γ_{12} bands. Electronic Raman scattering from the essentially filled Γ_{12} bands would be very weak then, resulting in very little interference with Raman scattering from the phonons.

IV. CONCLUSION

We have extended our earlier Raman scattering study to the nontransforming $A15$ compounds V$_3$Ge and Nb$_3$Sb, thereby suppressing any effect of tetragonal microdomains on the Raman spectra. This also allows comparison of the Raman spectra from $A15$ compounds whose Fermi level progressively moves away from the Γ_{12} bands. We found an anomaly in V$_3$Ge that is similar to, but weaker than, that seen in V$_3$Si and Nb$_3$Sn. Electronic interactions with the E_g and T_{2g} phonons in Nb$_3$Sb are greatly suppressed, the phonons exhibiting simple anharmonic damping and fully symmetric line shapes. Correlation of the E_g phonon linewidths in V$_3$Si, Nb$_3$Sn, and V$_3$Ge with the magnetic susceptibility led us to propose that the dominant damping mechanism in these compounds consists of interband processes wherein the E_g mode decays into electron-hole pairs in the very flat bands emanating from the Γ_{12} level. A simple model of the interaction and of the joint density of states of the Γ_{12} bands is able to account quantitatively for the linewidth temperature dependence. These results are in accord with the recent conclusions of Weber and Mattheiss[28] that dimerization of the transition-metal sublattice is the primary driving mechanism for the martensitic transition.

Several improvements could be made to our simple model of the E_g phonon linewidth. We have neglected the effect of phonon lifetime broadening of the electronic energy levels on the Γ_{12} bands. This effect is expected to be linear in temperature and may be as large as 0.3–0.4 eV at room temperature in Nb$_3$Ge and Nb$_3$Al.[54] It is conceivable that a reduction in lifetime broadening upon cooling could provide the observed increase in E_g phonon damping. Pickett[55] has recently shown that such interactions may significantly alter the thermal distribution function $f(E)$ used in computing thermal averages. A more detailed theoretical calculation based on our model of the E_g phonon linewidth, and the use of realistic energy bands and incorporating lifetime broadening, would be highly desirable both to substantiate our model and to determine the relative significance of this last point.

*Present address: Department of Physics, University of Michigan, Ann Arbor, Michigan 48109.

[1]J. Labbé and J. J. Friedel, J. Phys. Radium 27, 708 (1966).

[2]L. P. Gorkov, Zh. Eksp. Teor. Fiz. Pis'ma Red. 17, 525 (1973) [JETP Lett. 17, 379 (1973)]; Zh. Eksp. Teor. Fiz. 65, 1658 (1973) [Sov. Phys.—JETP 38, 830 (1974)].

[3]L. P. Gorkov and O. N. Dorokhov, J. Low Temp. Phys. 22, 1 (1976); Zh. Eksp. Teor. Fiz. Pis'ma Red. 21, 656 (1975) [JETP Lett. 21, 310 (1975)].

[4]R. W. Cohen, C. D. Cody, and J. J. Halloran, Phys. Rev. Lett. 19, 340 (1967).

[5]J. Noolandi and L. J. Sham, Phys. Rev. B 8, 2468 (1973).

[6]E. Pytte, Phys. Rev. Lett. 25, 1176 (1970).

[7]B. M. Klein and J. L. Birman, Phys. Rev. Lett. 25, 1014 (1970).

[8]T. K. Lee and J. L. Birman, Phys. Rev. B 17, 4931 (1978).

[9]L. F. Mattheiss, Phys. Rev. 138, A112 (1965); Phys. Rev. B 12, 2161 (1975).

[10]R. N. Bhatt and W. L. McMillan, Phys. Rev. B 14, 1007 (1976).

[11]R. N. Bhatt, Phys. Rev. B 16, 1915 (1977).

[12]R. N. Bhatt, Phys. Rev. B 17, 2947 (1978).

[13]R. N. Bhatt, Phys. Rev. B 19, 4023 (1979).

[14]R. N. Bhatt and P. A. Lee, Phys. Rev. B 16, 4288 (1977); 17, 4129(E) (1978).

[15]H. Wipf, M. V. Klein, B. S. Chandrasekhar, T. H. Geballe, and J. H. Wernick, Phys. Rev. Lett. 41, 1752 (1978).

[16]S. B. Dierker, R. Merlin, M. V. Klein, B. S. Chandrasekhar, and J. W. Blue, preceding paper, Phys. Rev. B 27, 3571 (1983).

[17]S. Schicktanz, R. Kaiser, W. Spengler, and B. Seeber, Solid State Commun. 28, 935 (1979).

[18]S. Schicktanz, R. Kaiser, E. Schneider, and W. Gläser, Phys. Rev. B 22, 2386 (1980).

[19]B. M. Klein, L. L. Boyer, D. A. Papaconstantopoulos, and L. F. Mattheiss, Phys. Rev. B 18, 6411 (1978).

[20]A. T. van Kessel, H. W. Myron, and F. W. Mueller, J. Less-Common Met. 62, 49 (1978).

21Warren E. Pickett, K. M. Ho, and Marvin L. Cohen, Phys. Rev. B 19, 1734 (1979); K. M. Ho, Warren E. Pickett, and Marvin L. Cohen, *ibid.* 19, 1751 (1979); Phys. Rev. Lett. 41, 580 (1978).

22B. M. Klein, D. A. Papaconstantopoulos, and L. L. Boyer, in *Superconductivity in d- and f-Band Metals*, edited by H. Suhl and M. B. Maple (Academic, New York, 1980), p. 455.

23Pui K. Lam and Marvin L. Cohen, Phys. Rev. B 23, 6371 (1981).

24B. M. Klein, L. L. Boyer, and D. A. Papaconstantopoulos, J. Phys. F 8, 617 (1978).

25L. F. Mattheiss and W. Weber, Phys. Rev. B 25, 2248 (1982).

26B. M. Klein, L. L. Boyer, and D. A. Papaconstantopoulos, Phys. Rev. Lett. 42, 530 (1979).

27M. Kataoka, Phys. Lett. 80A, 35 (1980).

28W. Weber and L. F. Mattheiss, Phys. Rev. B 25, 2270 (1982).

29G. Shirane and J. D. Axe, Phys. Rev. B 4, 2957 (1971).

30S. A. Alterowitz, E. J. Haughland, D. E. Farrell, B. S. Chandrasekhar, J. W. Blue, and D. C. Liu, Phys. Rev. B 24, 90 (1981).

31R. Merlin, S. B. Dierker, M. V. Klein, J.-E. Jørgensen, S. E. Rasmussen, Z. Fisk, and G. W. Webb, in Proceedings of the International Conference on Phonon Physics, Bloomington, Indiana, 1981, edited by W. E. Bron [J. Phys. (Paris) Colloq. 42, C6-392 (1981)]

32J. H. Wernick, G. W. Hull, T. H. Geballe, J. E. Bernardini, and E. Buehler, J. Cryst. Growth 47, 73 (1979).

33A. V. Skripov, A. P. Stepanov, V. A. Marchenko, V. M. Pan, and A. D. Shevchenko, Zh. Eksp. Teor. Fiz. 77, 2313 (1979) [Sov. Phys.—JETP 50, 1113 (1979)]; V. M. Pan, V. C. Prokhorov, A. D. Shevchenko, G. A. Takzei, and M. Yurish, Fiz. Nizk. Temp. 4, 262 (1978) [Sov. J. Low Temp. Phys. 4, 130 (1978)]; V. M. Pan, A. D. Shevchenko, V. G. Prokhorov, and V. A. Marchenko, Zh. Eksp. Teor. Fiz. Pis'ma Red. 25, 141 (1977) [JETP Lett. 25, 129 (1977)].

34B. Pietrass, A. Handstein, and G. Behr, Phys. Status Solidi B 98, 597 (1980).

35E. Hegenbarth and B. Schmidt, Phys. Status Solidi B 76, 307 (1976).

36M. V. Klein, in *Light Scattering in Solids III*, edited by M. Cardona and G. Güntherodt (Springer, Berlin, 1982), p. 121.

37S. B. Dierker, M. V. Klein, J.-E. Jørgensen, and S. E. Rasmussen (unpublished).

38S. B. Dierker and M. V. Klein (unpublished).

39L. Pintschovious, H. G. Smith, N. Wakabayashi, W. Reichardt, G. W. Webb, and Z. Fisk, in *Superconductivity in d- and f-Band Metals, Karlsruhe, 1982*, edited by W. Buckel and W. Weber (Kernforschungszentrum Karlsruhe, Karlsruhe, 1982), p. 9.

40G. Shirane and J. D. Axe, Phys. Rev. Lett. 27, 1803 (1971).

41A. Akhiezer, J. Phys. (Moscow) 1, 277 (1939).

42R. T. Beyer and S. V. Letcher, in *Physical Ultrasonics* (Academic, New York, 1969), p. 255.

43L. R. Testardi, in *Physical Acoustics*, edited by W. P. Mason and R. N. Thurston (Academic, New York, 1973), Vol. X, p. 193.

44L. R. Testardi and T. B. Bateman, Phys. Rev. 154, 402 (1967).

45N. Toyota, T. Fukase, M. Tachiki, and Y. Muto, Phys. Rev. B 21, 1827 (1980).

46A. V. Skripov, A. P. Stepanov, V. M. Pan, A. D. Shevchenko, and I. G. Michailov, Phys. Status Solidi B 102, 671 (1980).

47J. P. Maita and E. Bucher, Phys. Rev. Lett. 29, 931 (1972).

48A. M. Clogston and V. Jaccarino, Phys. Rev. 121, 1357 (1961).

49W. Rehwald, M. Rayl, R. W. Cohen, and G. D. Cody, Phys. Rev. B 6, 363 (1972).

50G. W. Webb, Z. Fisk, and D. C. Johnston, Phys. Lett. 73A, 350 (1979).

51F. Cerdeira, T. A. Fjeldly, and M. Cardona, Phys. Rev. B 8, 4734 (1973).

52J. B. Hastings, G. Shirane, and S. J. Williamson, Phys. Rev. Lett. 45, 1249 (1979).

53L. J. Sham (private communication).

54P. B. Allen, W. E. Pickett, K. M. Ho, and M. L. Cohen, Phys. Rev. Lett. 40, 1532 (1978).

55W. E. Pickett, Phys. Rev. Lett. 48, 1548 (1982).